Journal of Southeast University (English Edition) Vol. 24, No. 1, pp. 46 – 49 Mar. 2008 ISSN 1003—7985

Application of wavelet package filtering in the de-noising of fiber optic gyroscopes

Wang Qi Xu Xiaosu

(School of Instrument Science and Engineering, Southeast University, Nanjing 210096, China)

Abstract: To reduce the drift error existing in the output signal of fiber optic gyroscopes (FOG), a mathematical model of the FOG output signal is set up; the error characteristics of the FOG output signal are analyzed, and semi-soft threshold filtering is chosen based on the comparison of hard threshold and soft threshold filtering. The semi-soft threshold wavelet package filtering method is applied in the filtering of the FOG output signal. Experiments of the stationary and dynamic FOG output signals filtered with the wavelet package analysis are carried out in a lab environment, respectively. Experiments done with the real-time measured FOG signal show that the method of semi-soft threshold wavelet package filtering reduces the mean square error from 5 (°)/h to 1 (°)/h, so it is effective in eliminating the white noises and the fractal noises existing in the FOG. The novel method proposed here is proved valid in reducing the FOG drift error, satisfying the technical demands of high precision and real-time processing.

Key words: wavelet package analysis; signal processing; fiber optic gyro; threshold filtering

It is important to determine the carrier azimuth angle and the attitude angle accurately and quickly in a strapdown inertial navigation system. Gyro drift is the most important factor that affects the accuracy of a strapdown inertial navigation system. How to eliminate the gyro drift effectively is an essential problem to guarantee the strapdown inertial navigation system accuracy[1]. The gyro drift is classified into systematic drift and random drift. The systematic drift can be eliminated by a satisfactory mathematical model and drift compensation calculation. The random drift composed of white noises and fractal noises is weak nonlinear, slow time invariant and is often affected by some indeterminate factors such as exterior environmental noise. Traditional methods to compensate for the random drift are not effective in the strapdown inertial navigation system.

There is much colored noise in the gyro random drift, such as fractal noises characterized by non-stationary, long-term dependence and self-similarity. If a traditional filter is used to process the noise, the complexity will increase and other errors will be introduced simultaneously. Wavelet analysis is especially suitable for non-stationary fractal signal processing and with relatively good filtering results. In this paper, the wavelet package transform is utilized to perform multi-resolution analysis in gyro signals. Good filtering results are obtained by the wavelet package filtering method which has already been applied in practical engineering systems.

1 Wavelet Analysis of FOG Signal

Time-domain presentation of the FOG signal, in which form the signals are usually provided, does not show the signal properties except for their variations over time. On the other hand, frequency representations of the signal shows different frequency components existing in the signal, including the vehicle dynamics, white and colored noises, and long-term as well as short-term errors. To overcome the shortcomings of the Fourier transform and the inverse Fourier transform, the wavelet transform (WT) analyzing the localized area of a large signal with a variable-sized window is adopted in the analysis of the FOG signal. The WT is capable of providing the time and frequency information simultaneously, thus, giving a time-frequency representation of the signal. Stretching or compressing the window width is referred to as scaling a wavelet. Long time interval windows are used where a precise low frequency component is needed and short intervals where high frequency information is considered. Usually, the low frequency contents of the signal are the most important parts of it that identify the signal trend and are capable of providing very good approximations about the signal. The approximations correspond to the high scale low frequency part. On the other hand, the high frequency contents correspond to the low scale high frequency part. Therefore, a wavelet multi-resolution analysis is performed based on the approximation and details provided using the WT. The wavelet multi-resolution analysis decomposes the FOG signals into both coarse resolution, which contains information about low frequency components and retains the main features of the original signal, and fine resolution with information about the high frequency components. Furthermore, this process is reversible as the signal reconstruction is defined as the summation of the final approximation components and the detail components of all levels.

1.1 Wavelet transform

The wavelet transform was originally used to approximate a signal of a function using a set of functions, called a wavelet basis, which is provided by the mother wavelet. Wavelets are a family of basis or basis-like functions formed by dilation and translation of the mother wavelet function $\psi(x)$:

$$\psi_{(a,b)}(x)=\frac{1}{\sqrt{a}}\psi\left(\frac{x-b}{a}\right) \tag{1}$$

Received 2007-06-08.

Biographies: Wang Qi (1981—), male, graduate; Xu Xiaosu (corresponding author), male, doctor, professor, xxs@seu.edu.cn.

Foundation items: Pre-Research Program of General Armament Department during the 11th Five-Year Plan Period (No. 51309020503), the National Defense Basic Research Program of China (973 Program) (No. 973-61334), the National Natural Science Foundation of China (No. 50575042), Specialized Research Fund for the Doctoral Program of Higher Education (No. 20050286026).

Citation: Wang Qi, Xu Xiaosu. Application of wavelet package filtering in the de-noising of fiber optic gyroscopes[J]. Journal of Southeast University (English Edition), 2008, 24(1): 46 – 49.

where $\psi(x)$ is a function in $L^2(\mathbf{R})$ and satisfies the following mathematical requirements:

$$C_\psi = \int_{\mathbf{R}^*} \frac{|\hat{\psi}(\omega)|^2}{|\omega|} \mathrm{d}\omega < \infty \tag{2}$$

where $\mathbf{R}^* = \mathbf{R} - \{0\}$ represents nonzero real numbers. Wavelets are used to represent data or other functions. Projection of the signal onto a wavelet basis function is called a wavelet transform. The wavelet transform is defined as

$$W_{\mathrm{f}}(a, b) = \int_{\mathbf{R}} f(x) \bar{\psi}_{(a,b)}(x) \mathrm{d}x = \frac{1}{\sqrt{a}} \int_{\mathbf{R}} f(x) \bar{\psi}\left(\frac{x-b}{a}\right) \mathrm{d}x \tag{3}$$

where the parameters a and b represent the scale and shift of the wavelets. With the value of parameter a decreasing, the time window width of $\psi_{(a,b)}(x)$ decreases and the main frequency increases. It can detect high frequency components. In contrast, with the value of a increasing, the time window width of $\psi_{(a,b)}(x)$ increases and the main frequency decreases. It can detect the low frequency components.

1.2 Wavelet package analysis

The wavelet transform offers superior temporal resolution of the high-frequency components and the scale resolution of the low-frequency components[2-3]. But wavelet transform analysis introduces another problem that is called "lower frequency resolution in the higher frequency band and lower time resolution in the lower frequency band". The wavelet package transform has succeeded in overcoming this deficiency.

Unlike the wavelet transform, which only decomposes the low frequency components of the immediate upper level, the wavelet package transform decomposes the low frequency and high frequency bands simultaneously and can enhance the frequency resolution of the processing signal. Figs. 1(a) and (b) show the differences between the wavelet transform and the wavelet package transform[4-5].

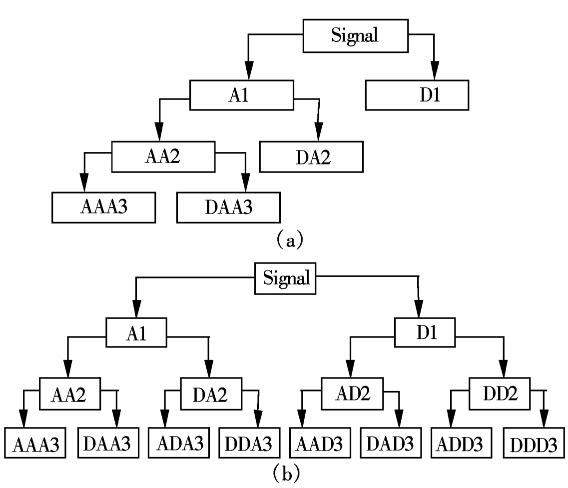

Fig. 1 Difference between the wavelet transform and the wavelet package transform. (a) Structure of wavelet analysis; (b) Structure of wavelet package analysis

Using the symbol:

$$\mu_0(t) = \varphi(t), \quad \mu_1(t) = \psi(t) \tag{4}$$

where $\varphi(t)$ and $\psi(t)$ are the scale function and the wavelet function, respectively. The series of functions defined by Eq. (4), $\{\mu_l(t); l = 0, 1, 2, \ldots\}$, is called the wavelet package of the scale function $\varphi(t)$.

$$\left.\begin{aligned} \mu_{2l}(t) &= \sqrt{2} \sum_{n \in \mathbf{Z}} h_n u_l(2t - n) \\ \mu_{2l+1}(t) &= \sqrt{2} \sum_{n \in \mathbf{Z}} g_n u_l(2t - n) \end{aligned}\right\} \tag{5}$$

For any $m \geqslant 0$ and $j \in \mathbf{Z}$,

$$U_j^m = \mathrm{closespan}\{\mu_{m,j,k}(t) = 2^{\frac{j}{2}} \mu_m(2^j t - k); k \in \mathbf{Z}\}$$

According to the properties of the wavelet package, it can be deduced that

$$U_j^{2m} \perp U_j^{2m+1}, \quad U_{j+1}^m = U_j^{2m} \oplus U_j^{2m+1}$$

When $W_j(j \geqslant 2)$, the subspace of $L^2(\mathbf{R})$ is decomposed. It can be expressed as[6]

$$W_j = U_{j-1}^0 \oplus U_{j-1}^1 = U_{j-2}^0 \oplus U_{j-2}^1 \oplus U_{j-2}^2 \oplus U_{j-2}^3 = \ldots = U_0^{2^j} \oplus U_0^{2^j+1} \oplus U_0^{2^j+2} \oplus \ldots \oplus U_0^{2^{j+1}-1} \tag{6}$$

In other words, retaining the same time scale of W_j, $\Delta = 2^{-j}$ with p level wavelet package, the frequency band $H_j = [2^{j+1}\Delta\Psi, 2^{j+2}\Delta\Psi]$ corresponding to function sub-space W_j is further subdivided into at most 2^p sub-frequency bands. Therefore, the frequency resolution of the time-frequency analysis is greatly improved.

2 Process of De-noising of the FOG Signal with Wavelet Package Analysis

The method of wavelet package de-noising described here was principally developed by Donoho and Johnstone. The derivation from this method was proposed in Refs. [7-8], and the results are presented here for completeness.

$$y(t) = f(t) + n(t) \tag{7}$$

Consider the true signal $f(t)$ with the random drift $n(t)$ as functions at time t_i to be sampled, $i = 1, 2, \ldots, n$.

Let $W(\cdot)$ and $W^{-1}(\cdot)$ denote the forward and inverse wavelet transform operators. Then the de-noised signal $\hat{f}(t)$ can be written as

$$\hat{f}(t) = W^{-1} T_\lambda W(f)$$

where T_λ denotes the de-noising operator with threshold $\lambda = \sigma\sqrt{2\ln N}$ for the wavelet package transform. There are usually two types of thresholding operators: soft and hard threshold functions.

$$T_\lambda^{\mathrm{hard}}(p) = \begin{cases} 0 & |p| < \lambda \\ p & |p| \geqslant \lambda \end{cases} \tag{8}$$

$$T_\lambda^{\mathrm{soft}}(p) = \begin{cases} 0 & |p| < \lambda \\ \mathrm{sign}(p)(|p| - \lambda) & |p| \geqslant \lambda \end{cases} \tag{9}$$

where p is the coefficient of the decomposition.

$$T^{\text{semi}}_{t_1,t_2}(p)=\begin{cases}0 & |p|\leqslant t_1\\ \operatorname{sgn}(p)\dfrac{t_2(|p|-t_1)}{t_2-t_1} & t_1<|p|\leqslant t_2\\ p & |p|>t_2\end{cases}\qquad(10)$$

where sgn(∗) is the sign function; usually t_2 can be chosen as $t_2=\sigma\sqrt{2\ln N}$; the choice of t_1 is determined in the form of the signal. The semi-soft threshold function can increase the effect of the wavelet transform. After comparing many threshold functions, the following function is selected as the threshold function in this paper.

$$T^{\text{semi}}_{t_1,t_2}(p)=\begin{cases}0 & |p|\leqslant 0.5\sigma\sqrt{2\ln N}\\ \operatorname{sgn}(p)\dfrac{t_2(|p|-t_1)}{t_2-t_1} & 0.5\sigma\sqrt{2\ln N}<|p|\leqslant\sigma\sqrt{2\ln N}\\ p & |p|>\sigma\sqrt{2\ln N}\end{cases}\qquad(11)$$

This method works in four steps in the case of wavelet package transform de-noising[9]:

① Transform the noisy data into the wavelet domain using a wavelet package function;

② Choose an entropy criterion to select the best basis;

③ Apply semi-soft threshold coefficients smaller than a certain amplitude;

④ Reconstruct the data.

3 Analyses of FOG Error Characteristic and Error Model

Considering the features of different error sources in Fig. 2, it can be summarized that the noises can ultimately be divided into white Gaussian noises, power law noises (1/f noise and random walk noise) and biasing drift (especially referring to temperature drift)[10-11]. The FOG error sources and the characteristics are shown in Fig. 2.

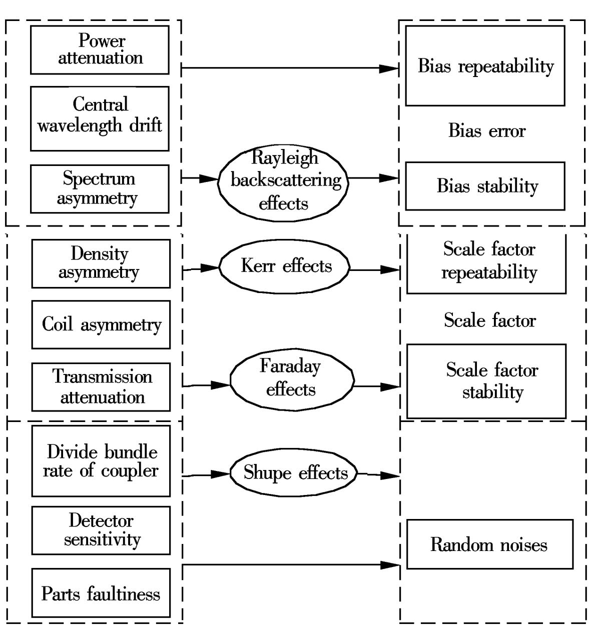

Fig. 2 FOG error sources and error characteristics

In the experiment, an FOG was put on a stationary-base platform. The measuring axis of the FOG was placed horizontally.

From the error characteristic analysis, the FOG output signal can be modeled as

$$\omega(t)=\omega_{\mathrm N}\cos K+\varepsilon_0+A\sin(2\pi f+\theta_0)+x(t)+W(t)+T(t)\qquad(12)$$

where $\omega(t)$ is the real output of the FOG; $\omega_{\mathrm N}=\omega_{ie}\cos\phi$ is the northern part of the earth rotation rate; ϕ is the latitude; K is the angel between the measurement axis of the FOG and the geographic north; ε_0 stands for the zero-bias of the FOG, which can be regarded as a constant in short time; A, f, θ_0 stand for the amplitude, frequency and the initial phase of periodical parts in the output signal, respectively; $x(t)$ is the fractal noise; $W(t)$ stands for the zero-mean white noise; $T(t)$ is the temperature associated output signal.

4 Simulation Results from FOG

The methods of de-noising the FOG measure include FIR filtering, IIR filtering, time series analysis, multi-sensor information fusion, and wavelet analysis, etc. Limited by the effects and the real-time of these processing methods, many methods cannot be applied in the technical projects. The wavelet package analysis with the semi-soft threshold filtering method is suitable for processing the fractal noises and the white noises existing in the FOG output signal.

FOG F92I02 is put on the Type SMT-Ⅰ three-axis rotation platform, and the FOG output is a stationary signal while the rotation platform is stationary. The drift signal shown in Fig. 3 is from the measurement of the IFOG F92I02 and has been processed by the wavelet transform algorithm, where the db5 wavelet basis is selected. The signal sampling frequency is 50 Hz. The original signal and the wavelet package transformed signal are shown in Fig. 3. After the wavelet package transform, the standard variance of the signal decreases from 5 to 1 (°)/h.

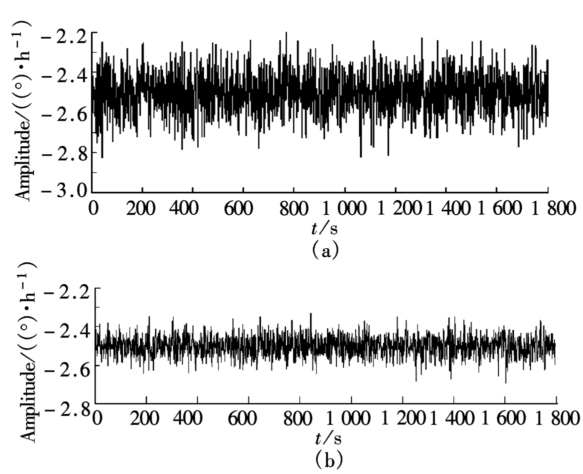

Fig. 3 De-noising effect comparison of the static drift signal.
(a) The original signal; (b) The wavelet package transformed signal

Put the IFOG F92I02 on the SMT-Ⅰ Type three-axis rotation platform, and the FOG output is a dynamic signal while the rotation platform turns at a certain fixed rate. The results of the wavelet transform of the dynamics are shown in Fig. 4.

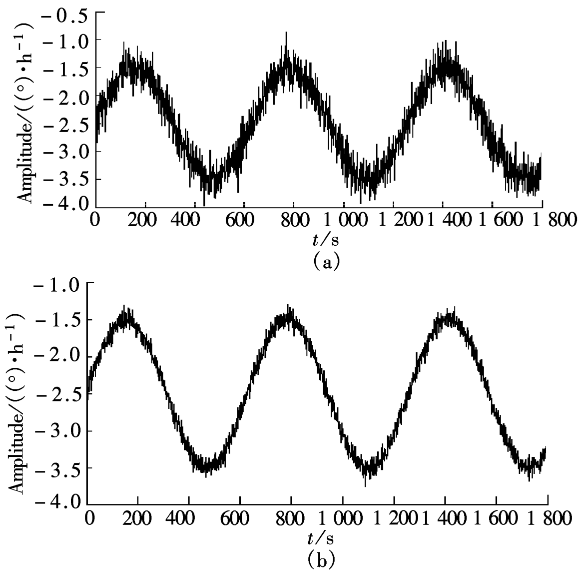

Fig. 4 De-noising effect comparison of the dynamics signal. (a) The original dynamic signal; (b) The wavelet package transformed dynamic signal

5 Conclusion

A semi-soft threshold wavelet package transformation algorithm is analyzed in detail based on the analysis of the wavelet package analysis and the error characteristics of the FOG output signal. A fitful semi-soft threshold function is selected after many tries in the wavelet package reconstruction. Simulation experiments of the real-time acquired FOG measurement verify the validity of the algorithm proposed. The algorithm has already been implemented in the floating point DSP TMS320VC33 and the technical needs can be satisfied.

References

[1] Ji Xunsheng, Wang Shourong, Xu Yishen. Application of fast wavelet transformation in signal processing of MEMS gyroscope [J]. *Journal of Southeast University*: *English Edition*, 2006, **22**(4): 510 − 513.

[2] Chen Xiyuan. Modeling random gyro drift by time series neural networks and by traditional method[C]//*IEEE International Conference on Neural Networks and Signal Processing*. Nanjing, China, 2003: 810 − 813.

[3] Rajagopal K, Singh B, Singh B, et al. Novel methods of temperature compensation for permanent magnet sensors and actuators [J]. *IEEE Transactions on Magnetics*, 2001, **37**(4): 1995 − 1997.

[4] Han Junlian, Ge Shengmin, Shen Yi, et al. Modeling and simulation of digital closed-loop fiber optic gyroscope[C]//*The 6th World Congress on Intelligent Control and Automation*. Dalian, China, 2006: 1659 − 1663.

[5] Gao Yukai, Deng Zhenglong. Extraction of FOG signal from fractal noise[C]//*IEEE International Conference on Neural Networks & Signal Processing*. Nanjing, China, 2003: 768 − 771.

[6] Sun Feng, Luo Chao, Gao Wei, et al. Research on modeling and compensation method of fiber optic gyro random error [C]//*IEEE International Conference on Mechatronics & Automation*. Niagara, Canada, 2005: 461 − 465.

[7] Schneider M. Filters and algorithms for rotation rate detection in fiber optic gyroscopes[J]. *IEEE Transactions on Aerospace and Electronic Systems*, 1994, **30**(2): 511 − 517.

[8] Wang Xinlong, Jin Zhenshan, Shen Gongxun, et al. Using a neural network learning algorithm suitable for the best estimation of nonlinear system[C]//*The 4th World Congress on Intelligent Control and Automation*. Shanghai, China, 2002: 2030 − 2034.

[9] El-Sheimy Naser, Chiang Kai-Wei, Noureldin Aboelmagd. The utilization of artificial neural networks for multisensor system integration in navigation and positioning instruments [J]. *IEEE Transactions on Instrumentation and Measurement*, 2006, **55**(5): 1606 − 1615.

[10] Shu Xiaowu, Liu Cheng. The research of digital close-loop depolarized FOG[C]//*The 3rd World Congress on Intelligent Control and Automation*. Hefei, China, 2000: 1473 − 1477.

[11] Nugroho Anto Satriyo, Kuroyannagi Susumu, Iwata Akira. FOG forecasting using self growing neural network "CombNET-Ⅱ"—a solution for imbalanced training sets of problem [C]//*IEEE-INNS-ENNS International Joint Conference on Neural Networks*. Como, 2000: 429 − 434.

小波包变换滤波在光纤陀螺信号降噪处理中的应用

王 其 徐晓苏

(东南大学仪器科学与工程学院,南京 210096)

摘要:为了减小光纤陀螺仪输出信号中的漂移误差,对小波变换和小波包变换进行了理论分析和比较,建立了光纤陀螺仪输出信号的数学模型,分析了其输出信号的误差特性,在详细分析比较硬阈值和软阈值小波滤波的基础上,提出了采用半软阈值作为滤波阈值.并在实验室环境下分别对光纤陀螺静态和动态输出数据进行了半软阈值小波包滤波实验.对光纤陀螺实时测量信号的实验结果表明:采用半软阈值小波包滤波方法对光纤陀螺仪输出数据进行处理,静态和动态输出信号误差均方差可以从5 (°)/h减少到1 (°)/h,有效地消除了光纤陀螺仪中白噪声和分形噪声的影响.该方法比小波滤波方法更加有效地消除了光纤陀螺漂移误差的影响,且能够满足光纤陀螺仪输出高精度和实时处理的要求.

关键词:小波包变换;信号处理;光纤陀螺仪;阈值滤波

中图分类号:TP206⁺.1